Electrical Power and Energy Systems 115 (2020) 105499

Contents lists available at ScienceDirect

Electrical Power and Energy Systems

journal homepage: www.elsevier.com/locate/ijepes

Improving the autonomy of islanded microgrids through frequency regulation

Yuri Rodrigues[a,*], Maíra Monteiro[a,b], Morad Abdelaziz[a], Liwei Wang[a], Antonio Z. de Souza[b], Paulo Ribeiro[b]

[a] School of Engineering, University of British Columbia, Kelowna, Canada
[b] Institute of Electrical Systems and Energy, Federal University of Itajuba, Itajubá, Brazil

ARTICLE INFO

Keywords:
Conservation frequency reduction
Energy storage systems
Frequency dependency
Islanded microgrid autonomy

ABSTRACT

In stand-alone operation, microgrids are susceptible to potential shortages in generation capacity, requiring a consideration of all technically feasible opportunities to conserve energy in order to keep the islanded grid operational for as long as possible. In this sense, the network autonomy capacity must be considered in the islanded microgrid frequency control formulation, alongside the traditional concern related to the accomplishment of the dynamic frequency regulation requirements. This paper proposes a new outlook for secondary frequency regulation in islanded microgrids denoted as conservation frequency reduction (CFR). The proposed approach exploits the frequency dependency characteristics of microgrids by intentionally reducing the reference setpoint of the islanded network frequency in a controllable way in order to decrease the network's demand and improve the autonomy duration of islanded microgrids, i.e., availability to supply demand in islanded mode; while ensuring the system operation within permissible limits. The results indicate that the proposed approach is able to significantly enhance islanded microgrids autonomy capacity while guaranteeing its frequency of operation within satisfactory dynamic and steady-state limits.

1. Introduction

The continuous expansion of distributed energy resources (DERs) and the increasing interest in the improvement of power system reliability have significantly promoted the development of microgrids. Microgrids are defined as electric regions comprising a group of loads and DERs with well-defined electric boundaries having local controllability and capable of operating connected to the main grid and/or in stand-alone mode (i.e., islanded) [1,2]. These regions are able of significantly improving the system's reliability, locally performing controls previously held at the transmission level during abnormal circumstances such as failures in the main grid, scheduled maintenance and other unpredicted events that could otherwise lead to the interruption of the supply [1,4]. In these environments frequency regulation measures are required during dynamic and steady-state operating conditions including fluctuations in load, variations of uncontrolled renewable generation, unpredicted events, etc. [3]. For this, additional consideration to the traditional methods employed at transmission level are necessary due to the particular characteristics of the islanded microgrids, especially the reduced availability of generating resources.

The initial efforts providing the definition of microgrids frequency control were proposed in [3]. This work establishes the hierarchical division of microgrids frequency regulation in three levels: primary regulation responsible for fast stabilizing control actions; secondary regulation in charge of returning the system to steady-state reference level of operation; and tertiary control seeking the economic dispatch of DERs. For primary regulation, there is a general consensus in the literature about the use of droop control as it only uses local feedback signals and does not require any communication network [4]. For secondary frequency regulation, several methods have been proposed in the literature to tackle additional characteristics relevant to islanded microgrids frequency regulation, [5,9,12,13]. In [5] a formal conceptualization of centralized and distributed secondary control strategies considering the traditional AGC perspective is proposed for stand-alone microgrids operation. New techniques seeking to ensure precise active/reactive power sharing among microgrids DERs are developed in [6,7]. These works respectively developed a consensus-based frequency regulation and adaptive virtual impedance. With the aim to the improve of frequency control realization time, a finite-time observer is proposed in [8] to estimate the overall information necessary for secondary

* Corresponding author.
E-mail address: yuri.rodrigues@ubc.ca (Y. Rodrigues).

https://doi.org/10.1016/j.ijepes.2019.105499
Received 6 May 2019; Received in revised form 15 August 2019; Accepted 19 August 2019
Available online 30 August 2019
0142-0615/ © 2019 Elsevier Ltd. All rights reserved.

Nomenclature

H	inertia constant
ΔP_G	generation contribution
ΔP_L	variations in the system demand
D	damping coefficient
$\omega(\omega^{\oplus})$ $(\omega_0^{\oplus})$	operating (setpoint) (reference value) frequency
Γ_k	DER governor control
m_k	DER droop constant
$\tau_{k,\langle\Gamma\rangle}$	governor time constant
$\mathcal{G}_\Gamma$	set of DERs
η	harnessing factor
$\bar{\Delta\omega}(\underline{\Delta\omega})$	maximum admissible frequency variation upper (lower) boundary
t^∞	system stabilization time
$\Delta\omega_\rho$ $(\Delta\omega_\alpha)$	primary (CFR-AGC) frequency deviation
$\mathrm{P}_{\mathrm{N},\alpha}$, (P_N)	active power contribution by the proposed CFR-AGC (traditional secondary controllers)
$k_P(k_I)$	proportional (integral) secondary controller PI compensator
$u_k^\omega(u_k^p)$	frequency (active power) control inputs
$u_k^{\omega,\langle P\rangle}(u_k^{\omega,\langle I\rangle})\left(u_{k,\int}^{\omega,\langle I\rangle}\right)$	proposed controller proportional (integral) parcel
$k_\omega(k_E)$	reconnection (available energy) compensator
E $(\bar{\mathrm{E}})(\underline{\mathrm{E}})$	current (maximum) (minimum) available energy
δ_k	rotor electrical angular position
ω_s	synchronous frequency
$P_k^e(P_k^m)$	turbine electrical (mechanical) power
$P_k^{m,\oplus}$	reference setting of the turbine mechanical power
$T_{k\langle\rho\rangle}$	turbine time constant
$\mathcal{M}_k$	synthetic-inertia constant
$\mathcal{N}_k$	set of buses connected to node k
$P_{j\text{-k}}^e$	active power flowing from node j to k
t_0	time of event
k_{pf} (k_{qf})	active (reactive) power frequency sensitivity
E_s	microgrid instantaneous energy savings
0 (1)	matrix with all elements valued as 0's (1's)

regulation to speed-up the microgrid stabilization. The consideration of plug-in electric vehicles (PEV) as energy storage systems (ESS) for frequency regulation support is developed in [9], while [10,11] discuss the control requirements to enable PEV and ESS applications for grid support. Microgrids dynamic performance during frequency regulation is addressed in [12,13]. The work in [12] proposes the use of bounded control inputs to mitigate the transient overshoot during frequency regulation, whereas [13] benefits from microgrids advanced monitoring systems based on distributed-level phasor measurement units (D-PMU) to develop an adaptive frequency controller able to speed-up the system frequency recovery speed and mitigate oscillations. These approaches are mainly focused on the realization of microgrid operation at frequency reference level.

On another avenue, initial developments towards the flexibilization of microgrids frequency of operation were proposed in [14,16]. These works allow for islanded networks operation at lower frequency levels seeking to reduce the necessary amount of frequency responsive reserves for primary regulation in multi-microgrid (MMG) systems. In [14] a reduction in islanded microgrids frequency of operation is proposed to decrease the requirements for governor responsive reserves from renewable DERs. A hierarchical energy management system for MMG systems is proposed in [15] seeking to increase each microgrid maximum load variation capacity, without the need for further expansions in primary regulation capabilities. Next, [16] develops an autonomous power sharing strategy for MMG system towards the improvement of microgrid's stability margin. For this, in case of load variations in a weaker microgrid a neighboring system can compensate these variations allowing for a general improvement of the operating range of the MMG systems frequency reserves. In spite of the fact that the works in [14,16] provided important contributions towards the flexibilization of microgrids frequency of operation, there are several aspects pertaining to the aforementioned literature that still require additional attention and further developments: (1) The adopted modeling is limited and may not be feasible for real environments, i.e., the available works are only aware of steady-state frequency realization considering primary regulation, which is typically not sufficient for ensuring the system stability during transients especially as microgrids have very limited inertia capacity; (2) The modeling of generators is oversimplified and lack sufficient representation of the respective frequency controller's dynamics required to achieve the microgrid steady-state frequency operational level; (3) There is no actual control exerted to determine the amount of reduction in the system operating frequency level. Instead, the flexibilization of the microgrid frequency of operation is provided by the natural frequency deviation obtained after primary droop frequency regulation; (4) The control strategy may not be feasible for real environments, as successive load increases or large disturbances, e.g. islanding and loss of generation, can lead to significant steady-state frequency offsets after primary regulation, which would yield limits violation; In this perspective, (5) secondary control actions are required to ensure the system operation within permissible limits; In addition, (6) none of the previous works have considered the possibilities enabled by microgrids frequency of operation flexibilization to improve the autonomy of stand-alone networks with limited availability of generation, i.e. duration of islanded operation. The last represents one of the major challenges to ensure islanded microgrids steady-state operation in environments where local generation capacity is limited to the existing stored energy, i.e. energy storage-based microgrids.

In this perspective, seeking to address the aforementioned limitations and to establish the necessary conditions to exploit the new opportunities enabled by the islanded microgrid operation, wherein the system is isolated from the main grid and the reference frequency can be assigned locally depending only on the loads tolerance to frequency deviations [17], this paper proposes the concept of conservation frequency reduction (CFR). The proposed approach adaptively determines the adequate frequency operating condition for an islanded microgrid based on the locally available energy resources. For this, a novel perspective for automatic generation control (AGC), i.e. secondary control, in islanded microgrids denoted CFR-AGC is developed. It is demonstrated that by adaptively regulating a microgrid's operating frequency setpoint it is possible to effectively reduce the network demand, improving the service-time of the available energy storage systems (ESS), and as a result significantly enhance the network survival time, while still keeping the system operating within the permissible limits. To validate the proposed control, dynamic analysis and modeling were developed for two test system. First, the IEEE 34-bus test system was employed to demonstrate the proposed approach feasibility and its ability to improve islanded microgrids autonomy capacity. Next, the IEEE 123-bus was used showcasing the proposed approach applicability to large microgrid environments considering multiple generating units enclosed in different generating groups. The main contribution of this work to the state-of-art of islanded microgrids operation are following described:

- Improvement of microgrids dynamic modeling for flexible frequency operation analysis: A detailed modeling of generators dynamics, primary and secondary regulation is included. In contrast to the available approaches in the literature, where generators dynamics are disregarded, considering only a linearized swing (balance) equation.

- Enhancement of islanded microgrids autonomy capacity through frequency regulation: This work tackles the frequency regulation process to improve microgrids autonomy capacity. To this end, this work proposes the concept of conservation frequency reduction (CFR), where the frequency deviation is used to provide long-term energy savings due to the microgrid frequency damping. On the other hand, existing works available in the literature addressing frequency flexibilization are mainly focused on the reduction of the necessary frequency responsive reserves for MMG systems, i.e. primary regulation, and do not consider the possible long-term energy savings potential.
- Controllable flexibilization of microgrids operating frequency setpoint: The proposed CFR-AGC provides secondary control actions, intentionally controlling the reduction in islanded microgrids frequency of operation. This significantly improves the ability to harness microgrids frequency reduction and the applicability of the current approaches in real microgrid environments with significant demand variations.
- Adaptive CFR-AGC harnessing factor: The proposed CFR-AGC strategy is associated with an adaptive harnessing factor. The proposed factor uses the availability of local energy resources and the expected reconnection time to adaptively determine the most effective microgrid frequency operating level. In this sense, the proposed CFR-AGC strategy is still effective even in cases where an optimistic reconnection period is initially expected by the system operator and does not occur, where in such cases the proposed adaptive harnessing factor is able to re-adjust the islanded network's frequency as time goes by in a way that still allows for improvements in the microgrid autonomy capacity.

2. Frequency regulation for islanded microgrids

In stand-alone configuration, microgrids lose the frequency reference signal of the main grid requiring local control strategies to maintain its operation and regulate its frequency within satisfactory limits [3,4]. Its frequency response can be generically denoted by (1) [13], being composed of four main parcels: (1) The first parcel represented by $\frac{1}{2H}$ gives the system inertial response, providing fast corrective actions to disturbances, where H is the inertia constant; (2) The second term ΔP_G depicts the microgrids generation contribution. It is responsible of securing the system generation/demand balance; (3) The third parcel denoted by ΔP_L depicts the disturbances caused by variations in the system demand; and (4) the fourth parcel $D\cdot(\omega(t) - \omega^{\oplus})$ represents microgrid's demand damping due to frequency dependency characteristics, where D is the damping coefficient, ω and $\omega^{\oplus}$ are the network operating- and reference- frequency. In this sense, given a perturbation in microgrids steady-state operation $\Delta P_L(t)$, frequency controllers must actuate dispatching the available generating resource, $\Delta P_G(t)$, in order to restore the system to an equilibrium condition, i.e. $\Delta\dot{\omega}(t) = 0$.

$$\Delta\dot{\omega}(t) = \frac{1}{2H}\cdot[\Delta P_G(t) - \Delta P_L(t) - D\cdot(\omega(t) - \omega^{\oplus})] \tag{1}$$

This process is traditionally performed in two main control steps, primary and secondary control. Primary frequency control is defined as the first level in the frequency control hierarchy. This control is typically held by the droop method [4], which provides a proportional corrective action based on frequency deviation to offset the power variation imposed by the disturbance that was initially supplied by the system inertial response. However, this control action leads to an unintentional steady-state frequency deviation, requiring the implementation of secondary control actions to return the system to a desirable frequency operating level. One should notice that this uncontrollable frequency deviation is used by the approaches proposed in [14,16] to develop their respective MMG frequency flexibilization strategies, which as indicated in [3] can be unfeasible for real microgrids, once microgrids operating with only primary regulation can lead to steady-state operative conditions violating the system permissible operative limits. In this perspective, secondary control actions must be performed.

Traditionally, secondary frequency regulation is held by centralized controllers denoted automatic generation control (AGC). These controllers are based on slow PI controls responsible to dispatch a selected group of generators to mitigate the system frequency offset, i.e. take over the load damping parcel, restoring the microgrid operation to reference frequency setpoint [18]. The complete microgrid frequency regulation process including primary and secondary levels are detailed illustrated in Fig. 1. It shows the respective power contributions from inertia response, frequency reserves and frequency damping for a given demand disturbance.

Where 'A' is defined as the pre-disturbance frequency, 'C' is the maximum frequency deviation after disturbance, i.e. nadir, 'B' is defined as the stabilizing frequency after primary regulation, 'D' is the time when secondary control is activated to return the system operation to the reference level.

In this perspective, considering the limitations of the literature state-of-art, wherein the available approaches would not exert actual control of the microgrid frequency damping, but instead take advantage of the unintentional frequency deviation due primary regulation [14,16]. This paper seeks to improve the state-of-art of microgrids frequency regulation, developing a novel secondary frequency controller able to intentionally harness, in a controllable way, the system

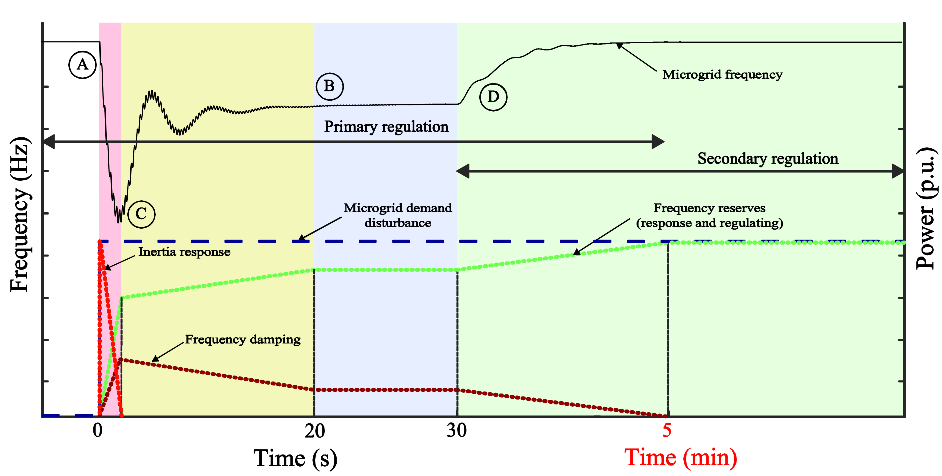

Fig. 1. Frequency regulation process.

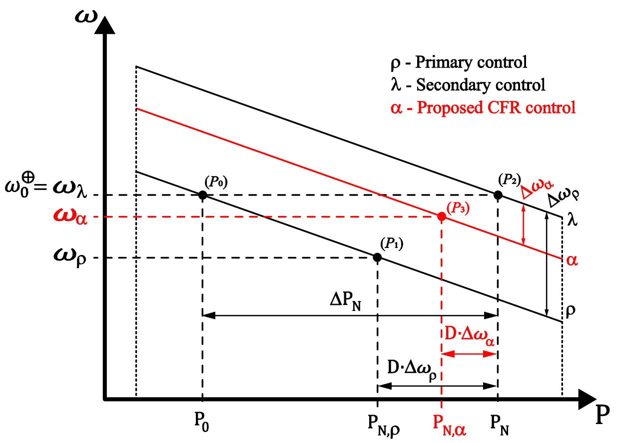

Fig. 2. Steady-state representation of the proposed CFR- and traditional- secondary frequency controller.

frequency damping to improve the islanded microgrid autonomy capacity, i.e., duration of islanded operation.

3. Proposed conservation frequency reduction control for islanded microgrids

In this section the proposed concept of conservation frequency reduction for islanded microgrids frequency regulation is depicted in details. This concept enables the development of a new frequency control outlook allowing for the frequency regulation of islanded microgrids within permissible limits, while intentionally offsetting the operational frequency level seeking the improvement of the system autonomy capacity.

3.1. Concept of conservation frequency reduction

Power system frequency of operation standards are developed in order to ensure that a high energy quality is available to the respectively supplied loads [19]. Still, this high-quality frequency level typically defined in 60/50 $\pm$ 0.1(Hz) range may not be necessary for islanded microgrids operation. During this operating mode the most sensitive and non-critical loads are usually disconnected in the early stages of operation, leaving the network with general loads that can be operated without such high-quality frequency requirements [17], i.e. a middle quality frequency of operation in the 60/50 $\pm$ 0.5(Hz) range may be assumed [14,15]. This enables a new perspective allowing for the flexibilization of microgrids' frequency of operation, motivating the proposed concept of conservation frequency reduction. The proposed concept seeks to adaptively adjust the microgrid frequency controller parameters based on the availability of local energy resources and expected reconnection time, determining the most adequate frequency of operation for the islanded microgrid to take advantage of microgrids frequency dependency. It is shown in this work that by adequately controlling the microgrid operating frequency it is possible to significantly improve microgrids islanded operating time in environments where the local generation capacity is restricted to the available stored energy.

3.2. Primary regulation

First, the traditional primary regulation based on droop control is considered (2), [13]. It delivers an automatic response within cycles after the disturbance, providing the frequency arrest and the initial generation/demand balance. The respective steady-state behavior of droop method is obtained from the linearization of (2), leading to the relation depicted in (3), [4]. From (3) one can observe that an unintentional steady-state frequency deviation proportional to the governor actuation is produced as an outcome of primary regulation. In this sense, secondary frequency control must be implemented for islanded microgrid regulation at a desirable frequency level.

$$\dot{\Gamma}_k(t) = -\frac{1}{\tau_{k,\langle\Gamma\rangle}}\cdot[\Gamma_k(t) + m_k{}^{-1}\cdot(\omega_k(t) - \omega^{\oplus})] \tag{2}$$

$$\Delta\omega = \omega^{\oplus} - \omega_k(t) = m_k\cdot\Gamma_k(t) \tag{3}$$

where Γ_k denotes the DER governor control, ω_k is the DER frequency, and $\tau_{k,\langle\Gamma\rangle}$ is the governor time constant and m_k depicts the DERs droop coefficient, $k \in \mathcal{G}_\Gamma$, where $\mathcal{G}_\Gamma$ denotes the set of DERs.

3.3. Secondary regulation

In view of the potential reduction of microgrids net demand supply due to the system frequency damping illustrated in Fig. 1, wherein the same amount of load is supplied requiring less generating power when the microgrid is operating at frequency levels lower than the reference value, from (1) one can conclude that $\{\Delta P_G(t) - D\cdot(\omega(t) - \omega^{\oplus})\} < \Delta P_L(t)|\omega(t) < \omega_0^{\oplus}$, where $\omega_0^{\oplus}$ denotes the system frequency reference value, typically 60- or 50 (Hz). This work proposes a novel perspective for secondary frequency regulation denoted by conservation frequency reduction (CFR). The proposed method adaptively adjusts the microgrid frequency setpoint introducing a harnessing factor denoted by η. This factor provides an intentional deviation in the operating frequency setpoint based on the availability of local generation. Seeking the system operation in a flexible equilibrium condition within permissible limits i.e. $\omega_0^{\oplus} \geq \omega(t) \geq (\omega_0^{\oplus} - \bar{\Delta\omega})|t \geq t^{\infty}$, where $\bar{\Delta\omega}$ denotes the microgrid maximum admissible frequency variation and t^{∞} denotes the system stabilization time.

The proposed CFR regulating process is depicted in Fig. 2. It includes a comparison with traditional secondary control perspective to highlight the enabled capacity of energy preservation by the proposed controller, i.e. traditional secondary frequency controllers operate with fixed frequency setpoint, $\omega^{\oplus} = \omega_0^{\oplus}$, pursuing the microgrid restauration to steady-state operation at frequency reference level, i.e. $\Delta\dot{\omega}(t) = 0,\ \omega = \omega^{\oplus}\ |t \geq t^{\infty}$.

Fig. 2 presents a microgrid initially operating in steady-state frequency reference level (P_0), when a load increase of ΔP_N leads to the system perturbation. This perturbation triggers primary control actions, leading to the system stabilization in a new operative condition denoted by (P_1), i.e.$\Delta\dot{\omega} = 0$. This adjustment comes with an unintentional frequency deviation $\Delta\omega_\rho$, which as indicated in the results of [13] may cause the microgrid operation in violation of the permissible steady-state operating limits, i.e. $\omega \notin [\omega_0^{\oplus} + \Delta\omega,\ \omega_0^{\oplus} - \bar{\Delta\omega}]$. This perspective is corrected by secondary control actions. Traditional secondary controllers would reestablish the system operation to the steady-state reference level, eliminating the system frequency damping as indicated in (P_2), i.e. $\Delta\dot{\omega} = 0,\ \omega = \omega_0^{\oplus}$. In contrast, the proposed approach seeks the microgrid operation at the most effective frequency level, within

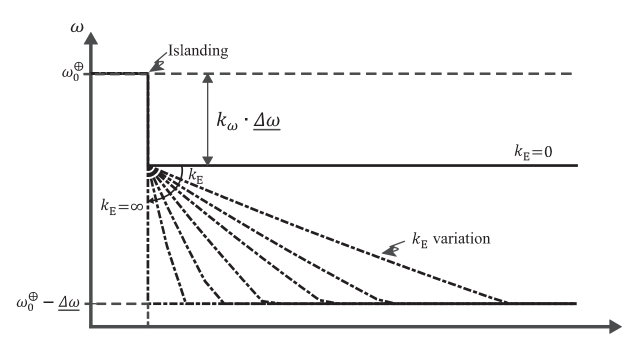

Fig. 3. Proposed adaptive CFR-AGC controller.

permissible limits, to harness the frequency damping characteristic as illustrated by (P_3), i.e. $\Delta\dot{\omega} = 0$, $\omega \in [\omega_0^{\oplus} + \Delta\underline{\omega}, \omega_0^{\oplus} - \Delta\bar{\omega}]$. This allows for the microgrid supplying of the same amount of load, however with reduced power consumption, i.e. $\mathrm{P}_{\mathrm{N},\alpha} \leq \mathrm{P}_{\mathrm{N}} | \mathrm{P}_{\mathrm{N},\alpha} = \mathrm{P}_{\mathrm{N}} + (\Delta\mathrm{P}_{\mathrm{N}} - \mathrm{D}\cdot\Delta\omega_{\alpha})$, where $\mathrm{P}_{\mathrm{N},\alpha}$ and P_{N} are the respective microgrid power contribution by the proposed CFR automatic generation controller (CFR-AGC) and traditional secondary controllers, $\Delta\omega_{\alpha}$ is the proposed CFR-AGC frequency deviation to reference level.

The proposed control formulation aiming at the preservation of local energy resources for improving the autonomy of the islanded network is following depicted. The proposed controller follows a similar control concept described in [5,12]. The formulation is obtained based on the traditional droop formulation (3) derivation. Next, a variable change is performed to eliminate the active power parcel. From (4), it comes that $u_k^{p}(t) = m_k^{-1}\cdot(\dot{\omega}_k^{\oplus} - \dot{\omega}_k)$, performing this change of variable, it yields the control formulation (5).

$$\dot{\omega}_k^{\oplus} = \dot{\omega}_k + m_k\cdot\dot{\Gamma}_k = \dot{u}_k^{\omega,\langle P\rangle}(t) + m_k\cdot u_k^{p}(t) \tag{4}$$

$$\omega_k^{\oplus}(t) = \omega_k^{\oplus}|_{t_0} + \int_{t_0}^{t} \dot{u}_k^{\omega,\langle P\rangle}(t) + u_k^{\omega,\langle I\rangle}(t)\cdot dt \tag{5}$$

where $\dot{u}_k^{\omega,\langle P\rangle} = \dot{\omega}_k$, $u_k^{\omega,\langle I\rangle} = (\dot{\omega}_k^{\oplus} - \dot{\omega}_k)$, and $\omega_k^{\oplus}|_{t_0} = \omega_0^{\oplus}$. In this sense, the main goal is to design the controller parameters $\dot{u}_k^{\omega,\langle P\rangle}$ and $u_k^{\omega,\langle I\rangle}$ to provide the ability to harness the frequency dependency in improving the autonomy of islanded microgrids, while also producing a reliable frequency regulation of the microgrid within permissible limits.

This perspective is modeled by (6)–(8) establishing a new steady-state frequency regulation outlook, where given an event at a time t_0, within a finite time $t^{\infty} \geq t_0$:

(1) The active power sharing error and frequency deviation to reference value are null:

$$\lim_{t\to t^{\infty}} |m_k\cdot[\Gamma_k(t) - \Gamma_k(t_0)] - m_i\cdot[\Gamma_i(t) - \Gamma_i(t_0)]| = 0 | \ \forall\ t \geq t^{\infty}, \{k, i\} \subset \mathcal{G}_{\Gamma} \tag{6}$$

$$\lim_{t\to t^{\infty}} |\omega_k(t) - \omega_k^{\oplus}| = 0 | \ \omega_k(t) - \omega_k^{\oplus} = 0,\ \forall\ t \geq t^{\infty},\ k \in \mathcal{G}_{\Gamma} \tag{7}$$

(2) The frequency operational level is controlled at a desired frequency deviation condition to reference level, $\Delta\underline{\omega}\cdot\eta$, enabling the controller to harness microgrid frequency dependency:

$$\lim_{t\to t^{\infty}} |\omega_k(t) - \omega_0^{\oplus}| = \Delta\underline{\omega}\cdot\eta | \ \omega_k(t) - \omega_0^{\oplus} = \Delta\underline{\omega}\cdot\eta,\ \forall\ t \geq t^{\infty},\ k \in \mathcal{G}_{\Gamma},\ \eta \in \mathbb{R}[0, 1] \tag{8}$$

To design this controller, the global frequency error is employed considering (6) and (7), where $u_k^{\omega,\langle P\rangle}(t) = u_k^{\omega,\langle I\rangle} = \omega - \omega^{\oplus}$. In addition, as this controller seeks to provide an intentional frequency deviation to harness microgrid frequency dependency, the frequency reference value is design considering (8). In this perspective, the microgrid

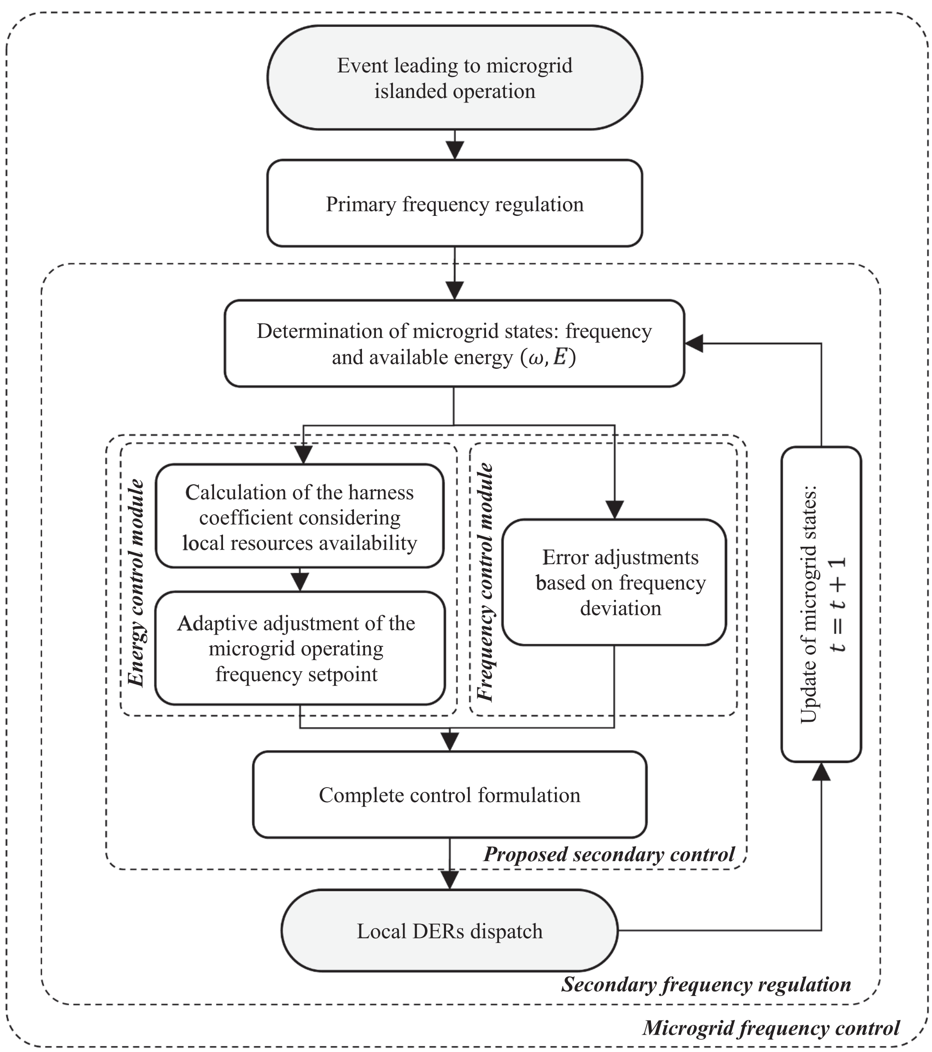

Fig. 4. Proposed controller flowchart.

operating frequency setpoint is represented as $\omega^{\oplus} = \omega_0^{\oplus} - \Delta\omega\cdot\eta$. This step introduces a new control stage denoted as energy control module, which is latter highlighted in the proposed control wholesale methodology illustrated in Fig. 4. The respective proposed frequency controller including the global frequency error and the adaptive harness factor can be compactly described by (9a)–(9c),

$$\omega_i^{\oplus}(t) = \omega_i^{\oplus}|_{t_0} + k_P\cdot u_k^{\omega,\langle P\rangle}(t) + \int_{t_0}^{t} k_I\cdot u_k^{\omega,\langle I\rangle}(t)\cdot dt \tag{9a}$$

$$u_k^{\omega,\langle P\rangle}(t) = u_k^{\omega,\langle I\rangle}(t) = \omega - (\omega_0^{\oplus} - \underline{\Delta\omega}\cdot\eta) \tag{9b}$$

The harness coefficient denoted by η consists of two main parcels. First, a step adjustment of the frequency setpoint is performed based on the expected reconnection time. This aspect is weighted by k_ω and should be set to provide a setpoint tuning proportional to the expected period of islanding; i.e., a fast reconnection should be characterized by a small reduction in the frequency setpoint. The second parcel, characterized by k_E, is based on the willingness to reduce the system power frequency quality and stability margin in view of the depletion of available energy resources. This share controls the reduction rate of the frequency setpoint due to the microgrid energy depletion. A description of the proposed frequency controller CFR-AGC detail depicting the harness coefficient behavior is shown in Fig. 3.

$$\eta = k_\omega + (1 - k_\omega)\cdot\left(\frac{\bar{E} - E}{\bar{E} - \underline{E}}\right)\cdot k_E,\ \forall\ k_\omega \in \mathbb{R}[0, 1],\ k_E=\{x \in \mathbb{R}\ |x \geq 0\} \tag{9c}$$

where E, $\bar{E}$ and $\underline{E}$ are the current-, maximum- and minimum- available energy.

It should be noted that the traditional secondary control, i.e. re-establishment of the system frequency to reference level, $\Delta\omega = 0$, is a particular case obtained for $\eta = 0$, $|\{k_\omega = 0,\ k_E = 0\}$. This setting should be kept during the initial stages and resumed prior reconnection to the main grid. In this perspective, in case that the fault/event is cleared and reconnection to the main grid is possible, the proposed control would be set up to the traditional secondary control mode, consequently both systems would be operating at the same frequency reference level during the reconnection process, $\Delta\omega = 0$. This allows for the reconnection process to be handled by any of the tradition microgrid reconnection strategies available in the literature, see for instance [20,21]. On the other hand, the solution leading to the maximum demand reduction, i.e. optimal setting for autonomy enhancement: $min\{\Delta P_G(t) - D\cdot(\omega(t) - \omega_0^{\oplus})\}|\omega_0^{\oplus} \geq \omega(t) \geq (\omega_0^{\oplus} - \underline{\Delta\omega})\ \forall\ t \geq t^{\infty}$, and presenting the highest vulnerability and loss of power quality is achieved for the system operation at the lower boundary of the permissible region, $\eta = 1\ |\{k_\omega \in \mathbb{R}[0, 1],\ k_E \to \infty\}$. The latter setting is denoted as CFR-OP and typically should only be approached as the system energy availability becomes scarce and/or reconnection is not expected over a long period.

The flowchart depicting the wholesale methodology of the proposed controller is presented in Fig. 4.

4. Dynamic system modeling

To validate the proposed approach technically feasibility, given the special interest in the influence on the frequency regulation and the respective time scales corresponding to the problem under investigation, dynamic analyses are performed. The system dynamics are modeled considering the concepts used in [22,23]. For this, synchronous generators are represented by a structure-preserving model including the governor dynamics incorporating the proposed adaptive secondary frequency controller (CFR-AGC). The synchronous generators dynamics are characterized by:

$$\dot{\delta}_k(t) = \omega_s\cdot(\omega_k(t) - \omega_0^{\oplus}) \tag{10a}$$

$$\dot{\omega}_k(t) = \frac{1}{2H_k}\cdot[P_k^m(t) - P_k^e(t) - D_k\cdot(\omega_k(t) - \omega_0^{\oplus})] \tag{10b}$$

$$\dot{P}_k^m(t) = \frac{1}{\tau_{k,\langle\rho\rangle}}\cdot[\Gamma_k(t) - (P_k^m(t) - P_k^{m,\oplus})] \tag{10c}$$

$$\dot{\Gamma}_k(t) = -\frac{1}{\tau_{k,\langle\Gamma\rangle}}\cdot[\Gamma_k(t) + m_k^{-1}\cdot(\omega_k(t) - \omega^{\oplus})] \tag{10d}$$

where ω_s is the synchronous frequency, $P_k^{m,\oplus}$, P_k^m and P_k^e are the turbine reference- and current- mechanical power and electrical power, $\tau_{k,\langle\rho\rangle}$ is the turbine time constant, δ_k is the rotor electrical angular position.

The updated governor response considering the proposed CFR-AGC is derived from (9a)–(9c) and (10d), being described by

$$\dot{\Gamma}_k(t) = -\frac{1}{\tau_{k.\langle\Gamma\rangle}}\cdot\left[\Gamma_k(t) + m_k^{-1}\cdot\left(\omega_k(t) - \left\{\omega_k^{\oplus}|_{t_0} + k_P\cdot u_k^{\omega,\langle P\rangle}(t) + k_I\cdot u_{k,\int}^{\omega,\langle I\rangle}(t)\right\}\right)\right] \tag{11a}$$

$$u_k^{\omega,\langle P\rangle}(t) = (\omega_k(t) - \omega_0^{\oplus}) + \underline{\Delta\omega}\cdot\left[k_\omega + (1 - k_\omega)\cdot\left(\frac{\bar{E} - E_{\langle ESS\rangle}(t)}{\bar{E} - \underline{E}}\right)\cdot k_E\right] \tag{11b}$$

$$u_{k,\int}^{\omega,\langle I\rangle}(t) = \omega_s^{-1}\cdot\Delta\delta_k(t) + \underline{\Delta\omega}\cdot\left[k_\omega + (1 - k_\omega)\cdot\left(\frac{\bar{E} - E_{\langle ESS\rangle}(t)}{\bar{E} - \underline{E}}\right)\cdot k_E\right] \tag{11c}$$

The ESS control is performed by local power controllers, typical ESS control structures are available in [11]. The proposed CFR controller sends the frequency reference signals to the power controllers that dispatch these units with the adequate power contribution and frequency operating level. ESSs modeling is performed considering the concepts presented in [23]. This model indicates that for inverter-based DERs operating in PQ mode, i.e. $\mathcal{M}_k = D_k = 0$, the influence of these units in the system stability can be neglected. Its reasoning is guaranteed by the results presented in [24] which demonstrate that inverter-based DER's current and voltage control dynamics does not meaningfully influence the DER power control as they take place in much faster time scales, being possible to integrate these equations into the power flow solution.

$$\mathcal{M}_k\cdot\dot{\omega}_k(t) = -D_k\cdot(\omega_k(t) - \omega_0^{\oplus}) + P_k^e(t) - \sum_{j\in\mathcal{N}_k} P_{j\text{-}k}^e \tag{12}$$

where $P_{j\text{-}k}^e$ is the active power flowing from node j to k. $\mathcal{N}_k$ is the set of buses connected to node k, P_k^e is the real power injection, $\mathcal{M}_k$ denotes the synthetic inertia constant.

The following feedback closed-loop state-space formulation depicts the complete system dynamic modeling considering the proposed control implementation.

$$\dot{x}(t) = A\cdot x(t) + \mathrm{B}_1\cdot u(t) + \mathrm{B}_2\cdot r(t) + \mathrm{B}_3\cdot v_1 + \mathrm{B}_4\cdot v_2 \tag{13a}$$

$$\begin{bmatrix} \Delta\dot{\delta} \\ \Delta\dot{\omega} \\ \Delta\dot{P}^m \\ \Delta\dot{\Gamma} \end{bmatrix} = \left(\begin{bmatrix} 0 & \psi & 0 & 0 \\ 0 & -\mathrm{D}\cdot\mathrm{H} & H & 0 \\ 0 & 0 & -\mathrm{T}_{\langle\rho\rangle} & \mathrm{T}_{\langle\rho\rangle} \\ -\mathrm{T}_{\langle\Gamma\rangle}\cdot\mathrm{M}\cdot K_I & -\mathrm{T}_{\langle\Gamma\rangle}\cdot\mathrm{M}\cdot(1-K_P) & 0 & -\mathrm{T}_{\langle\Gamma\rangle} \end{bmatrix}\right) \cdot\begin{bmatrix} \Delta\delta \\ \Delta\omega \\ \Delta P^m \\ \Delta\Gamma \end{bmatrix} + \begin{bmatrix} 0 \\ -\mathrm{H} \\ 0 \\ 0 \end{bmatrix}\cdot\Delta P^e + \begin{bmatrix} 0 \\ 0 \\ 0 \\ -\mathrm{M}\cdot\Psi \end{bmatrix}\cdot E_{\langle ESS\rangle} + \begin{bmatrix} 0 \\ 0 \\ 0 \\ -\mathrm{M}\cdot K \end{bmatrix}\cdot k_\omega \tag{13b}$$

where $\psi = \omega_s\cdot diag(1_{|\mathcal{G}_\Gamma|})$, $\mathrm{D} = diag(D_\mathrm{k}, \cdots, D_{|\mathcal{G}_\Gamma|})$, $\mathrm{H} = 2^{-1}\cdot diag(H_k^{-1}, \cdots, H_{|\mathcal{G}_\Gamma|}^{-1})$, $\mathrm{T}_{\langle\cdot\rangle} = diag(\tau_{k,\langle\cdot\rangle}^{-1}, \cdots, \tau_{|\mathcal{G}_\Gamma|,\langle\cdot\rangle}^{-1})$, $\mathrm{M} = diag(m_k^{-1}, \cdots, m_{|\mathcal{G}_\Gamma|}^{-1})$, $\mathrm{K}_I = -k_I\cdot\omega_s^{-1}\cdot diag(1_{|\mathcal{G}_\Gamma|})$,

$K_P = k_P \cdot diag(1_{|\mathcal{G}_\Gamma|})$, $\Psi = (k_P + k_I) \cdot \Delta\underline{\omega} \cdot (1\text{-}k_\omega) \cdot k_E \cdot diag(T_{\langle\Gamma\rangle})$, $E_{\langle ESS\rangle} = \sum_{k \in \mathcal{G}_{ESS}} \left(\frac{\bar{E}_k - E_k}{\bar{E}_k - \underline{E}_k} \right)$, $K = (k_P + k_I) \cdot \Delta\underline{\omega} \cdot diag(T_{\langle\Gamma\rangle})$, $\mathcal{G}_{ESS}$ is the set of ESS, 0's and 1's represent matrices of all zeros and ones with appropriate dimension, and $|\cdot|$ returns the cardinality of a respective setof interest.

5. Results

In this section the proposed secondary frequency controller based on conservation frequency reduction (CFR-AGC) is validated through case-studies simulations. The developed case-studies seek to demonstrate the improvement in the autonomy of islanded microgrids provided by the proposed harnessing factor based on the local availability of energy; evaluate whether the microgrid operation is kept within permissible limits; assess if adequate active power sharing is achieved between the generating units; and compare the islanded microgrids survival time considering the proposed method, traditional secondary control strategy and currently flexible frequency operation strategies available in the literature.

For this sake, two main case-studies are developed. The first case employs the IEEE 34-bus system modified to represent a microgrid capable of operating in stand-alone mode. The system represents a microgrid provided with local distributed generation (DGs), energy storage systems (ESS) and loads with frequency dependency characteristics [25]. The second case-study presents a large microgrid environment based on the IEEE 123-bus. In this case-study, different droop coefficients are used to evaluate the proposed controller ability to regulate multiple generating groups. For this, the respective modifications proposed in [13] for the inclusion of DGs in both test systems are considered. In addition, for each test systems different levels of ESS were associated. For IEEE 34-bus system each DG has 2 × 500 kVAh ESS associated, while for the IEEE 123-bus the associated ESS are based on the generators power sharing coefficient, ranging between 250 kVAh, 500 kVAh or 750 kVAh, e.g. for a generator with an $m_i = 0.05$ an ESS of 500 kVAh is associated. Operative limits established by the Brazilian ISO [19] are assumed and the proposed CFR-AGC controller settings are defined accordingly, where $\omega_0^{\oplus} = 60$ (Hz), $\underline{\omega} = 59.5$ (Hz), $\bar{E} = 100\%$, $\underline{E} = 0\%$, $k_P = 0.15$, $k_I = 0.17$, $k_E = 1.25$, $\bar{k}_\omega = 0.4$. Loads frequency dependency characteristics are given by $k_{pf} = 2.6$, $k_{qf} = 1.6$ [25], where k_{pf} and k_{qf} are loads active and reactive power frequency sensitivity. For each case-study five different control perspectives are considered to provide a comparison between the proposed CFR method and the literature state-of-art of frequency regulation, including: (1) the proposed CFR-AGC controller seeking to harness the microgrid frequency dependency while maintaining the best possible frequency quality in the expectation of reconnection in a foreseeable future; (2) the proposed controller in the optimal setting for autonomy enhancement, i.e. CFR-OP; (3) the key work on secondary control proposed in [5]; (4/5) state-of-art flexible frequency operation strategies [14] and [15].

5.1. Case-study IEEE 34-bus

This case study depicts the results obtained for the microgrid based on the IEEE 34-bus system. It is assumed that the system was initially operating connected to the main grid when a sudden disconnection occurs. Due to local generation limited capacity, maximum load shedding is performed leading to a total load of 3.07 p.u. representing the system most critical loads. To supply this load, an increase of 15% in the original local generation state prior islanding is required. DGs are dispatched up to their capacity limits suppling 91.25% of this load, with the residual demand met by ESS. In this perspective, once ESS are fully depleted the generation/demand balance will no longer be feasible, being the microgrid islanded operation terminated. This scenario requires energy preservation strategies to improve the islanded network autonomy. The obtained results for the literature and proposed CFR frequency controllers are depicted in Figs. 5 and 6 and Table 1.

Fig. 5 presents the microgrid dynamic- and steady-state frequency behavior. It enables one to determine the duration of islanded operation, the system frequency response accordance with the permissible dynamic and steady-state frequency limits, frequency oscillations, overshoot, and frequency nadir for the five different frequency control perspective, i.e. the proposed CFR-AGC, CFR-OP, the key work on secondary control proposed in [5] and the state-of-art flexible frequency operation strategies [14] and [15]. One can observe that after the system islanding, a significant frequency drop is featured leading to a system frequency nadir of 58.9 (Hz). During this period, primary regulation provides fast frequency control actions, stabilizing the system operation at 59.55 (Hz) past 20 (s) of disturbance. This behavior is similar among the analyzed controllers as their dissimilarities are associated with the second level of frequency regulation. At this moment, one can observe that the flexibilization of the microgrid frequency of operation in methods [14,15] is provided by the unintentional frequency deviation obtained after primary droop regulation. In this particular case-study, substantial energy savings are achieved due to the significant frequency deviation after primary regulation, enabling the enhancement of the microgrid autonomy operation at similar levels as the ones achieved by the proposed CFR method. However, the operational range of the methods in [14,15] shows to be very limited. For the respectively analyzed system, the maximum permissible load variation in which the microgrid remains operating within permissible frequency limits, i.e. $\omega \geq 59.5$ (Hz), is of 17%. This means that if

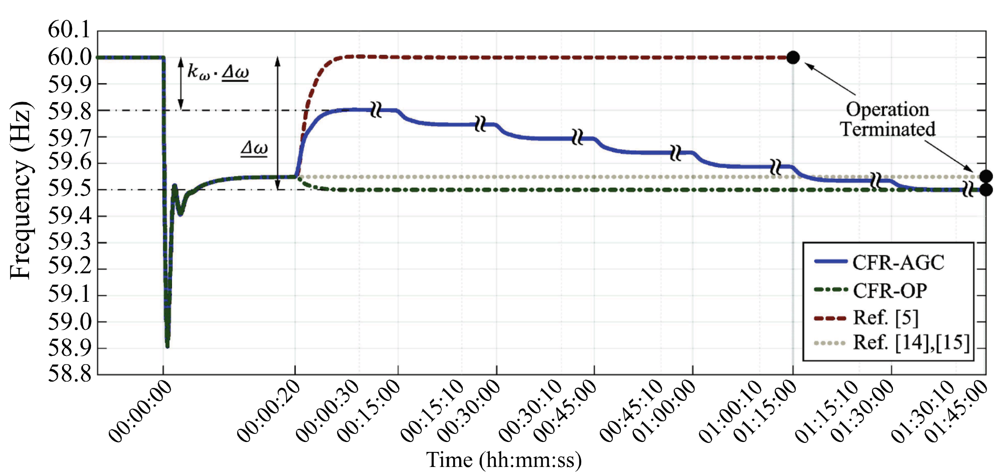

Fig. 5. Microgrid frequency response for CFR-AGC, CFR-OP, Refs. [5], [14] and [15] controllers – IEEE 34-bus.

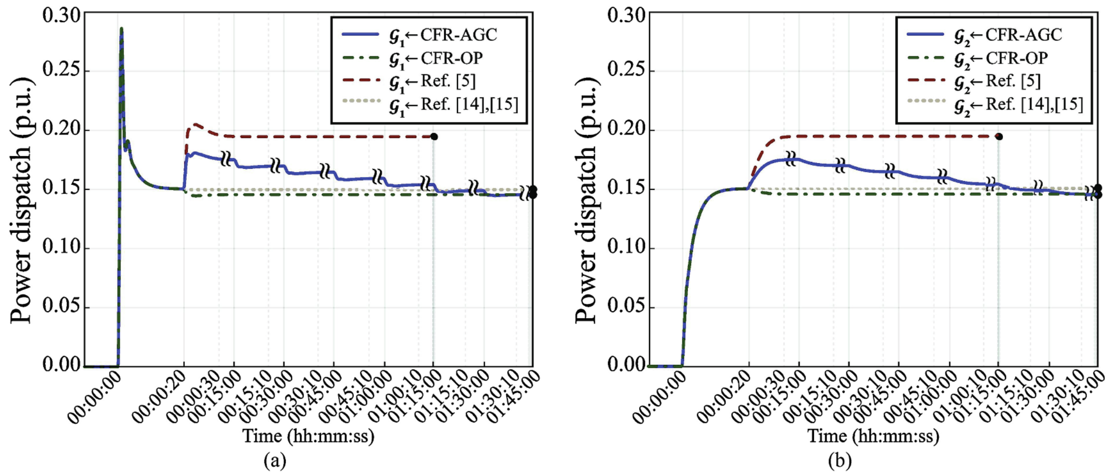

Fig. 6. Power dispatch for (a) $\mathcal{G}_1$; (b) $\mathcal{G}_2$; considering CFR-AGC, CFR-OP, Refs. [5], [14] and [15] controllers.

successive load increases or large disturbances, e.g. islanding and loss of generation, lead to a load variation greater than 17%, even though the system may have the necessary resources to reestablish its operation within permissible limits, due to the absence of secondary control capacity the microgrid would not be able to reestablish its operation within acceptable conditions, therefore limiting the applicability of the frequency flexibilization approaches [14,15] in microgrid environments with significant demand variation.

This limitation is overcome by the proposed CFR controllers and controller [5] through their embedded secondary control actions, triggering three different frequency behaviors as observed in Fig. 5. The controller developed in [5] seeks to resume the microgrid frequency of operation to reference level, i.e. 60 (Hz), sustaining this operating condition until the available energy resources are completely depleted, i.e. during 1:15 h. In contrast, the proposed CFR-AGC controller does not resume the system operation at reference level. It is able to adaptively determine the system frequency of operation, exerting an adaptive secondary frequency control in order to improve the system autonomy capacity while also seeking the best possible power quality. First, an initial improvement in the system frequency of operation to 59.8 (Hz) is performed. This occurs because the controller configuration was performed in the anticipation of a possible reconnection in a foreseeable future, therefore the frequency quality should be initially preserved. However, as time goes on and the microgrid local resources are reduced, the proposed CFR-AGC adaptive harnessing factor performs a progressive reduction of the network frequency of operation until the lower boundary of the permissible operating region is reached, i.e. 59.5 (Hz). The system operation is sustained in this condition until the generation/demand balance can no longer be achieved, leading to a total survival time of 1:45 h. In addition, looking towards the evaluation of the optimal energy preservation scenario, the proposed CFR-OP controller is also implemented. This controller immediately establishes the system operation at the maximum permissible frequency offset condition, i.e. 59.5 (Hz), maintaining this operating level until the full depletion of the available resources, which occurs past 1:45 h. The last configuration is recommended in cases where reconnection to the main grid is not expected before exhaustion of the locally available resources.

Based on these results, one can conclude that the flexibilization of microgrid frequency operation by the proposed CFR controllers and controllers [14,15] was able to uphold the islanded microgrid operational for additional 30 min in comparison to the traditional secondary control strategy proposed in [5]. These results represent an improvement of 40% in the system autonomy capacity. However, it should be noticed that the particularly expressive results obtained by [14,15] are due to the limited availability of local frequency responsive reserves in the small analyzed microgrid represented by the IEEE 34-bus system. In this sense, relatively small demand variations can leads to meaningful unintentional frequency deviation after primary regulation. Still, at the same time that this operating condition leads to expressive results, it also expose controllers [14,15] limitation due to the inability to regulate the desired operating frequency, i.e. in case that an additional load increase of 2% occurs, the microgrid operation should be terminated, as it would lead to the microgrid operation in violation of steady-state frequency limits, i.e. $\omega < 59.5$ (Hz). Therefore, limiting these controllers applicability for small microgrids with significant load variation. In addition, one should observe that the supplementary operational time enabled by CFR-AGC and CFR-OP controllers is similar. This occurs due to the harnessing factor ability to adaptively adjust the frequency levels based on the islanded network energy condition. In

Table 1
Microgrid response summary for CFR-AGC, CFR-OP, Refs. [5], [14] and [15] controllers - IEEE 34-bus.

	Time (hh:mm)	0:00	0:15	0:30	0:45	1:00	1:15	1:30	1:45
Ref. [5]	Energy available (kVAh)	1000.0	832.3	664.7	497.0	329.4	161.7	x	x
	Frequency setpoint (Hz)	60.0	60.0	60.0	60.0	60.0	60.0	60.0	60.0
Refs. [14,15]	Energy available (kVAh)	1000.0	867.07	733.41	599.75	466.10	332.44	198.78	65.12
	Frequency setpoint (Hz)	60.0	59.55	59.55	59.55	59.55	59.55	59.55	59.55
	Energy saving (kVAh)	–	139.1	135.9	135.9	135.9	135.9	135.9	135.9
CFR-AGC	Energy available (kVAh)	1000.0	849.4	700.8	556.5	416.3	280.1	147.9	17.9
	Frequency setpoint (Hz)	60.0	59.8	59.7	59.7	59.6	59.6	59.5	59.5
	Energy saving (kVAh)	–	68.3	76.3	93.3	109.8	125.9	141.6	150.8
CFR-OP	Energy available (kVAh)	1000.0	870.9	741.0	611.1	481.2	351.3	221.4	91.5
	Frequency setpoint (Hz)	60.0	59.5	59.5	59.5	59.5	59.5	59.5	59.5
	Energy saving (kVAh)	–	154.5	150.9	150.9	150.9	150.9	150.9	150.9

x – failure to meet the microgrid generation/demand balance.

this sense, even though the energy preservation achieved by CFR-OP was higher than the one provided by CFR-AGC, they were still in a similar range, not being enough to support an extra window of operation, i.e. 15 min.

The detailed description of the power supply can be assessed in Fig. 6(a)–(b). These results enable one to draw conclusions regarding the generators power contribution, controllers' ability to reduce the required power suppling, and the controllers' ability to guarantee adequate power sharing among the generating units. As one may observe, traditional secondary controller proposed in [5] leads to the highest power supplying requirement to meet the generation/demand balance, as the frequency damping is eliminated. In contrast, the proposed CFR controllers and [14,15] flexibilization of the islanded network operating frequency lead to meaningful reductions in the network demand, and consequently in the required supplying power, being the maximum reduction obtained by the proposed CFR-OP mode. It should be noticed that all methods were able to ensure adequate power sharing among the generating units (6) and (7).

An overall perspective of the obtained results is available in Table 1. It presents the available energy levels, operating frequency, and the respective instantaneous energy savings provided by the proposed CFR approaches and controllers [14,15] for each operating window of time. From Table 1, one can observe the direct relationship between the proposed CFR controllers' adjustment of the islanded microgrid operating frequency and the consequent energy savings. The total energy preservation provided by the proposed controllers harnessing of microgrid's frequency damping is obtained integrating the instantaneous energy savings along the operating time, $\int_{t_0}^{t^{\infty}} E_s(t)\cdot dt$, where $E_s(t)$ is the microgrid instantaneous energy savings. The total energy preservation enabled by the controllers CFR-AGC, CFR-OP and [14,15] are respectively 191 kVAh, 264 kVAh, and 239 kVAh. These additional reserves were able to provide the necessary energy to support 2 additional windows of operating, where in each window of operation the controllers depicted in Ref. [5], CFR-AGC, CFR-OP and Refs. [14,15] required a total of 167 kVAh, 151–130 kVAh, 130 kVAh, and 133 kVAh from the ESS to secure the system generation/demand balance.

5.2. Case-study IEEE 123-bus

In this section the proposed CFR controllers are validated considering the IEEE 123-bus system. This test system provides a large network environment where the feasibility of the proposed method can be stressed considering multiples generating groups, with different power sharing coefficients and ESS participation. For the simulations, similar conditions to the ones employed in the first case-study are assumed. After maximum load shedding, the islanded network requires an improvement of 20% of its local generation to ensure the microgrid generation/demand balance. Of this total, local generators are able to provide an additional 8%, with the remaining 12% generated by ESS. The results of this case-study are depicted in Figs. 7 and 8 and Table 2.

Fig. 7 illustrates the frequency behavior of a large microgrid during dynamic and steady-state operation. It allows one the determine the respective moment when the microgrid operation is terminated due to the failure to meet the generation/demand balance, evaluate whether the system operation is kept within permissible limits, and illustrates the differences in frequency responses of small and large microgrid environments. As one may observe in Fig. 7, differently from the first case-study depicted in Fig. 5, where a significant frequency drop is featured, in this case-study the microgrid frequency nadir is significantly lower, 59.7 (Hz), and the stabilized frequency of operation after primary regulation, 59.93 (Hz), remains close to the frequency reference level. These result are expected once the IEEE 123-bus system has a larger number of generators participating in the frequency regulation process, which significantly reduces the system frequency deviation during primary regulation. This leads to an opposite perspective for controllers [14,15], due to the large number of generating units participating in the primary regulation, the load variation, although at even higher levels than the first case-study, i.e. 20%, has not led to a significant frequency deviation after primary control stabilization, $\Delta\omega = 0.07$ (Hz). In this perspective, the proposed approaches in [14,15] were not able to meaningfully harness the system frequency damping capacity leading to the same operating time as the traditional secondary regulation [5]. In this perspective, one can conclude that the approaches [14,15] besides significantly restricting the operational range of small microgrids, as observed in the first case-study where the IEEE 34-bus islanded network operation is only allowed for small load variations, i.e. $\Delta P^e < 17\%$; their applicability to large microgrid environments with significant local generation as depicted by the IEEE 123-bus is also not efficient, as the large number of generating units participating in the primary regulation do not allow for a meaningful steady-state frequency deviation.

Further, given the small frequency deviation after primary stabilization, differently from the first case-study results depicted in Fig. 5, where the proposed CFR-AGC approach performed corrective actions seeking to improve the microgrid frequency of operation quality level from 59.55 (Hz) to 59.8 (Hz). Here, even though the controller possesses the same configuration, i.e., expects the microgrid reconnection in the foreseeable future, an opposite scenario from Fig. 5 is observed. The proposed CFR-AGC reduces the system operation from 59.9 (Hz) to 59.8 (Hz) seeking to improve the system energy preserving capacity. Additionally, the CFR-OP and the secondary controller proposed in [5] have similar behaviors to the first case-study as their configurations are independent of the system characteristics, i.e. the first respectively seeks the maximization of the system autonomy capacity leading to the network operation at the lower permissible boundary, i.e. 59.5 (Hz), while the second looks towards the system operation to the reference level, 60 (Hz). It should also be noted that in this case study, the

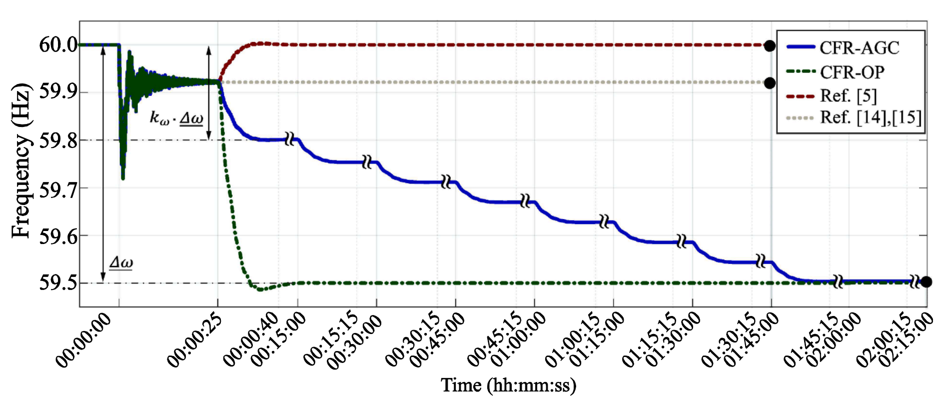

Fig. 7. Microgrid frequency response for CFR-AGC, CFR-OP, Refs. [5], [14] and [15] controllers – IEEE 123-Bus.

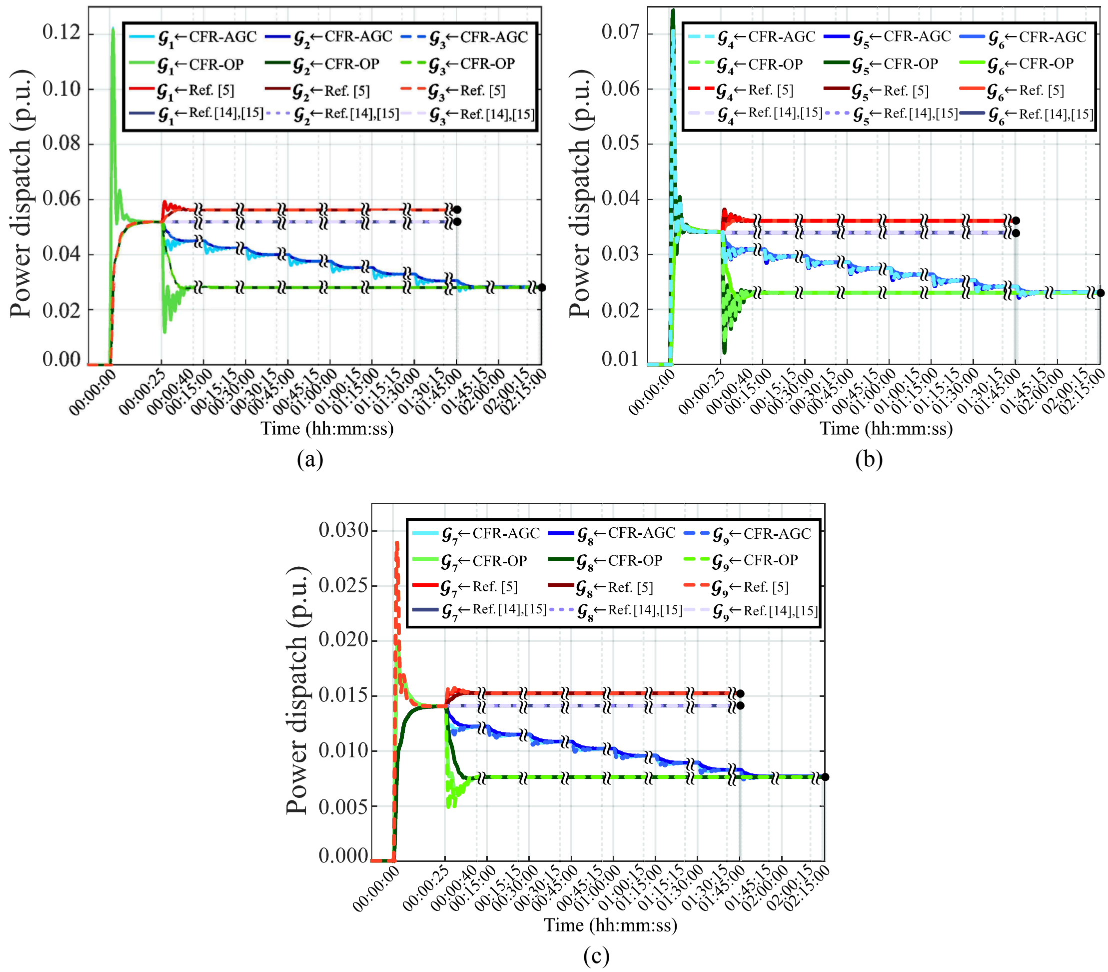

Fig. 8. Power dispatch for (a) $\{\mathcal{G}_1, \mathcal{G}_2, \mathcal{G}_3\}$; (b) $\{\mathcal{G}_4, \mathcal{G}_5, \mathcal{G}_6\}$; (c) $\{\mathcal{G}_7, \mathcal{G}_8, \mathcal{G}_9\}$; considering CFR-AGC, CFR-OP, Refs. [5], [14] and [15] controllers.

Table 2
Microgrid response summary for CFR-AGC, CFR-OP, Refs. [5], [14] and [15] controllers - IEEE 123-bus.

	Time (hh:mm)	0:00	0:15	0:30	0:45	1:00	1:15	1:30	1:45	2:00	2:15
Ref. [5]	Energy available (kVAh)	4500	3921	3343	2764	2186	1608	1029	451	x	x
	Frequency setpoint (Hz)	60.0	60.0	60.0	60.0	60.0	60.0	60.0	60.0	60.0	60.0
Refs. [14,15]	Energy available (kVAh)	4500	3936	3372	2808	2245	1681	1117	554	x	x
	Frequency setpoint (Hz)	60.0	59.93	59.93	59.93	59.93	59.93	59.93	59.93	59.93	59.93
	Energy saving (kVAh)	–	57.3	59.1	59.1	59.1	59.1	59.1	59.1	–	–
CFR-AGC	Energy available (kVAh)	4500	3963	3435	2917	2408	1908	1423	947	480	14
	Frequency setpoint (Hz)	60.0	59.8	59.8	59.7	59.7	59.6	59.6	59.5	59.5	59.5
	Energy saving (kVAh)	–	167	203	240	277	313	375	410	444	450
CFR-OP	Energy available (kVAh)	4500	4035	3569	3103	2637	2172	1706	1240	775	309
	Frequency setpoint (Hz)	60.0	59.5	59.5	59.5	59.5	59.5	59.5	59.5	59.5	59.5
	Energy saving (kVAh)	–	453	451	451	451	451	451	451	451	451

x – failure to meet the microgrid generation/demand balance.

proposed controller is once more able, due to the adaptive characteristic of the proposed harnessing factor, to achieve energy conservation levels similar to CFR-OP. The accomplished energy preservation led to the improvement of the microgrid autonomy capacity in two operative windows, i.e. 30 min, while ensuring the system operation within permissible limits during the complete analyzed period. This represented an increase of 29% in the microgrid duration of the islanded operation.

The microgrid power dispatch is depicted in Fig. 8(a)–(c) for each generating group. These figures depict the respective power dispatch of each unit contained in a respective generating group for each one of the analyzed controllers. The generating groups are constituted of 3 generating units with similar droop coefficients, i.e. power sharing capacity, and their associated ESS. In this perspective, analyzing the microgrid power dispatch in Fig. 8(a)–(c), one can observe a significant difference between each generating group power contribution. This occurs due to the different droop participation coefficients, where the first generating group depicted by $\{\mathcal{G}_1, \mathcal{G}_2, \mathcal{G}_3\}$ absorbed 57.1% of the dispatched power, while the second $\{\mathcal{G}_4, \mathcal{G}_5, \mathcal{G}_6\}$ and third $\{\mathcal{G}_7, \mathcal{G}_8, \mathcal{G}_9\}$ groups accounted respectively for 28.6% and 14.3%. Moreover, one should notice that all control methods were able to ensure an effective power sharing, i.e., all units enclosed in a same generating group provided an equal share of dispatched power at steady-state, even though the analyzed controller demanded different contributions.

A summary of the case-study results is depicted in Table 2. It presents the microgrid operating frequency level for each controller, the respective amount of available energy and the instantaneous energy savings enabled by the proposed CFR controllers and controllers [14,15]. Based on these results, one can identify that the proposed CFR-AGC and CFR-OP provide expressive total energy preservation, while controllers [14,15] are not able to meaningfully harness the system frequency dependency, the respective energy preservation levels are 720 kVAh, 1015 kVAh, and 118 kVAh. Additionally, the total energy requested from ESS to ensure the system generation/demand balance during each window of operation for each analyzed controller, i.e., Ref. [5], CFR-AGC, CFR-OP and Refs. [14,15], are respectively 578 kVAh, 537–466 kVAh, 466 kVAh and 564 kVAh.

6. Conclusion

Existing literature investigating islanded microgrid secondary frequency control have all presupposed a fixed reference level setpoint that remains constant throughout the entire islanded operation. In this paper, we amend this presupposition proposing an alternative approach denoted CFR-AGC that allows the frequency setpoint to change adaptively throughout the evolution of the microgrid islanded operation. Simulations were performed for small and large microgrid environments with multiple generators groups to validate the proposed method. The obtained results demonstrated that the adaptive adjustment of islanded microgrids operating frequency can significantly reduce the network power demand consumption, yielding significant improvements in the autonomy of islanded microgrids with limited energy resources. Moreover, these results highlights the importance of exerting actual control over the system frequency of operation. As observed, the current approaches available in the literature proposing microgrid's frequency flexibilization based on primary droop unintentional frequency deviation may not lead to actual improvement in the system autonomy in many islanded microgrid scenarios, and can also impose significant restrictions in the permissible demand variations in these islanded environments. Furthermore, the proposed controller provided effective power sharing and ensured the microgrid dynamic and steady-state operation within permissible limits. The results also indicate that even for configurations where the proposed CFR-AGC controller is adjusted based on optimistic scenarios, the adaptability of the proposed controller harnessing factor enabled the achievement of meaningful energy preservation levels similar to the ones obtained by the optimal autonomy capacity enhancement setting, CFR-OP. Based on these results, it is concluded that the proposed CFR-AGC provides a robust secondary frequency regulation strategy capable of significantly improving the autonomy of islanded microgrids. The main contributions of this work are following summarized.

- Expansion of islanded microgrids modeling for flexible frequency of operation analysis;
- Consideration of frequency regulation to improve the autonomy of islanded microgrids;
- Development of a novel secondary control perspective based on conservation frequency reduction (CFR-AGC), enabling a controllable flexibilization of microgrids operating frequency;
- Introduction of a harnessing factor able to adaptively determine the islanded network operating frequency based on the system available resources and expected reconnection time;

Declaration of Competing Interest

The authors declare that they have no known competing financial interests or personal relationships that could have appeared to influence the work reported in this paper.

Acknowledgements

This work was partially supported by CAPES, CNPQ, FAPEMIG, INERGE (Brazil) and NSERC (Canada). The author Yuri Rodrigues especially thanks CAPES Notice No. 18/2016 of the Full Doctoral Program Abroad/Process n° 88881.128399/2016-01, and the author Maíra Monteiro especially thanks CNPQ – Sandwich Doctorate Abroad/ Process n° 201128/2018/7.

References

[1] Lasseter RH. MicroGrids. IEEE power engineering society winter meeting, vol. 1. 2002. p. 305–8.
[2] Lasseter RH, Paigi P. Microgrid: a conceptual solution. PESC record - IEEE annual power electronics specialists conference, vol. 6. 2004. p. 4285–90.
[3] Lopes JAP, Moreira CL, Madureira AG. Defining control strategies for MicroGrids islanded operation. IEEE Trans Power Syst 2006;21(2):916–24.
[4] Olivares DE, et al. Trends in microgrid control. IEEE Trans Smart Grid 2014;5(4):1905–19.
[5] Shafiee Q, Guerrero J, Vasquez J. Distributed secondary control for islanded microgrids – a novel approach. IEEE Trans Power Electron 2014;29(2):1018–31.
[6] Guo F, Wen C, Mao J, Song Y. Distributed secondary voltage and frequency restoration control of droop-controlled inverter-based microgrids. IEEE Trans Ind Electron 2015;62(7):4355–64.
[7] Lou G, Gu W, Xu Y, Cheng M, Liu W. Distributed MPC-based secondary voltage control scheme for autonomous droop-controlled microgrids. IEEE Trans Sustain Energy 2017;8(2):792–804.
[8] Xu Y, Sun H. Distributed finite-time convergence control of an islanded low-voltage AC microgrid. IEEE Trans Power Syst 2018;33(3):2339–48.
[9] Pournazarian B, Karimyan P, Gharehpetian GB, Abedi M, Pouresmaeil E. Smart participation of PHEVs in controlling voltage and frequency of island microgrids. Int J Elec Power 2019;110:510–22.
[10] Rodrigues YR, de Souza ACZ, Ribeiro P. An inclusive methodology for Plug-in electrical vehicle operation with G2V and V2G in smart microgrid environments. Int J Elec Power 2018;102:312–23.
[11] Khodadoost Arani AA, Gharehpetian GB, Abedi M. Review on energy storage systems control methods in microgrids. Int J Elec Power 2019;107:745–57.
[12] Lu X, Yu X, Lai J, Wang Y, Guerrero J. A novel distributed secondary coordination control approach for islanded microgrids. IEEE Trans Smart Grid 2018;9(4):2726–40.
[13] Rodrigues YR, Abdelaziz M, Wang L. D-PMU based secondary frequency control for islanded microgrids. IEEE Trans Smart Grid 2019. [early access].
[14] Suh J, Yoon D, Cho Y, Jang G. Flexible frequency operation strategy of power system with high renewable. IEEE Trans Sust Energy 2017;8(1):192–9.
[15] Bui V, Hussain A, Kim Hak-Man. A strategy for flexible frequency operation of stand-alone multimicrogrids. IEEE Trans Sust Energy 2018;9(4):1636–47.
[16] Yoo H, Nguyen T, Kim H. Multi-frequency control in a stand-alone multi-microgrid system using a back-to-back converter. Energies 2017;10(6):822–40.
[17] Recommended practice for emergency and standby power systems for industrial and commercial applications, IEEE Std. 446-1995; 1996, p. 1–320.
[18] Frequency response initiative report, the reliability role of frequency response. EPRI; 2012.
[19] PRODIST Module 8 – energy quality, national electric energy agency (ANEEL) Std.; 2017.
[20] Rocabert J, Azevedo GMS, Luna A, Guerrero JM, Candela JI, Rodriguez P. Intelligent connection agent for three-phase grid-connected microgrids. IEEE Trans Power Electron 2011;26(10):2993–3005.
[21] Timbus A, Liserre M, Teodorescu R, Blaabjerg F. Synchronization methods for three phase distributed power generation systems - an overview and evaluation. IEEE 36th power electron spec conf. 2005. p. 2474–81.
[22] Cady S, Domínguez-García A, Hadjicostis C. A distributed generation control architecture for islanded AC microgrids. IEEE Trans Control Syst Technol 2015;23(5):1717–35.
[23] Guggilam S, Zhao C, Dall'Anese E, Chen Y, Dhople S. Optimizing DER participation in inertial and primary-frequency response. IEEE Trans Power Syst. 2018;33(5):5194–205.
[24] Mohamed Y, El-Saadany E. Adaptive decentralized droop controller to preserve power sharing stability of paralleled inverters in distributed generation microgrids. IEEE Trans Power Electron 2008;23(6):2806–16.
[25] Korunović LM, Milanović JV, Djokić SŽ, Yamashita K, Villanueva SM, Sterpu S. Recommended parameter values and ranges of most frequently used static load models. IEEE Trans Power Syst 2018;33(6):5923–34.